

Numerical Analysis of Four-Wave Mixing between 2 ps Mode-Locked Laser Pulses in a Tensile-Strained Bulk SOA

**Michael J. Connelly^a, Brendan F. Kennedy^b Douglas A. Reid^c
and Liam P. Barry^c**

- (a) Optical Communications Research Group, Department of Electronic
and Computer Engineering, University of Limerick, Ireland
- (b) Universidad de Santiago, Chile
- (c) Research Institute for Networks and Communications Engineering,
School of Electronic Engineering, Dublin City University, Ireland.



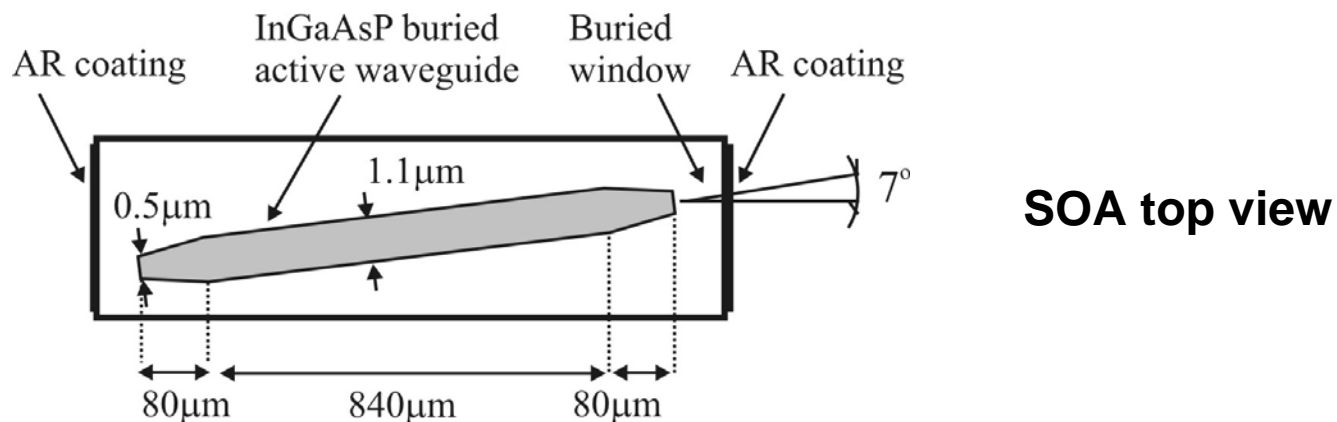
Outline

1. Introduction
2. Experiment
3. Pulse propagation model
4. Numerical algorithm and simulations
5. Conclusions

Introduction

- SOAs have attracted much interest for use in optical signal processing applications such as wavelength conversion.
- One of the most promising wavelength conversion mechanisms in an SOA is four-wave mixing (FWM).
- Transparent to modulation format and bit rate and has a wide conversion bandwidth.
- High conversion efficiency can be achieved by using narrow pump and probe pulses.
- Mathematical models of the FWM process occurring between two optical pulses in an SOA are required in order to design optical subsystems utilizing this process and also to enhance understanding of the FWM process itself.

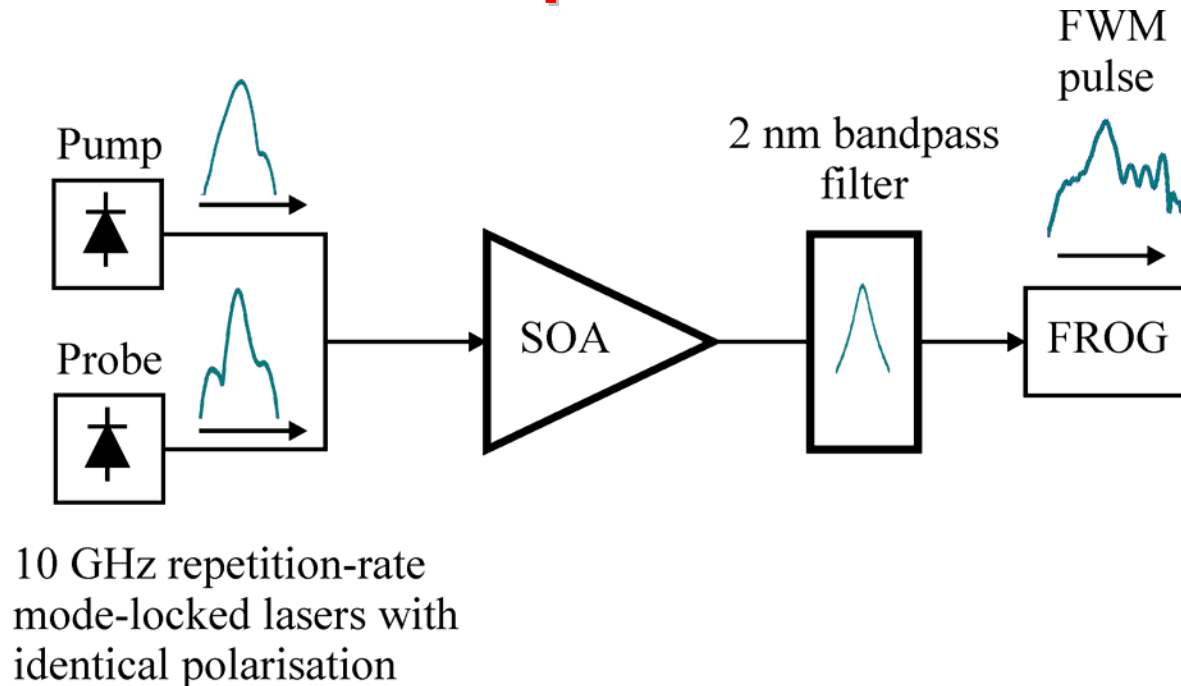
- We present numerical modelling and experimental results on the co-propagation of 10 GHz repetition rate picosecond mode-locked laser pump and probe pulses through a commercial tensile-strained bulk SOA* (Kamelian Ltd).



- The predicted FWM signal from the SOA model is compared with the pulse temporal profile obtained experimentally using the Frequency Resolved Optical Gating (FROG) technique.

C. Michie et al., *J. Lightwave Technol.*, 2006.

Experiment



FWM experiment

Pulse profiles measured using Frequency Resolved Optical Gating.

Model FWM process using the measured input pulses amplitude and phase and the bandpass filter response as model inputs.

Pulse Propagation Model

Use a modified Schrödinger equation (MSE) to model the pulse propagation*.

$$\left[\frac{\partial}{\partial z} + \frac{\gamma(\tau)}{2} + \left(\frac{\gamma_{2p}}{2} + ib_2 \right) |V(z,\tau)|^2 \right] V(z,\tau) = \left\{ \frac{1}{2} g_n(z,\tau) [1/f(\tau) + i\alpha_n(z,\tau)] + \frac{1}{2} \Delta g_T(z,\tau) [1 + i\alpha_T(z,\tau)] \right.$$

$$\left. - \frac{i}{2} \frac{\Gamma \partial g_m(z,\tau)}{\partial \omega} \Big|_{\omega_0} \frac{\partial}{\partial \tau} - \frac{1}{4} \frac{\Gamma \partial^2 g_m(z,\tau)}{\partial^2 \omega} \Big|_{\omega_0} \frac{\partial^2}{\partial \tau^2} \right\} V(z,\tau)$$

Annotations for the equation:

- Attenuation** (points to $\frac{\gamma(\tau)}{2}$)
- Direct effect of TPA** (points to $\frac{\gamma_{2p}}{2}$)
- Self-phase modulation** (points to ib_2)
- Saturated gain (carrier depletion)** (points to $\frac{1}{2} g_n(z,\tau)$)
- Dynamic gain (due to CH and TPA)** (points to $\frac{1}{2} \Delta g_T(z,\tau)$)
- 1st order gain dispersion** (points to $-\frac{i}{2} \frac{\Gamma \partial g_m(z,\tau)}{\partial \omega} \Big|_{\omega_0} \frac{\partial}{\partial \tau}$)
- 2nd order gain dispersion** (points to $-\frac{1}{4} \frac{\Gamma \partial^2 g_m(z,\tau)}{\partial^2 \omega} \Big|_{\omega_0} \frac{\partial^2}{\partial \tau^2}$)
- Complex pulse amplitude** (points to $V(z,\tau)$)
- Linewidth enhancement factors (carrier density changes & carrier heating)** (points to $i\alpha_n(z,\tau)$ and $i\alpha_T(z,\tau)$)

* M.Y. Hong et. al, *IEEE J. Quantum Electron.* 1994.

- In the model we also take into account the spatial and time dependency of the attenuation coefficient and linewidth enhancement factors.

Dynamic gain terms

...due to carrier heating ..due to stim. emission and free carrier absorption ..due to two-photon absorption

$$\Delta g_T(z, \tau) = - \int_0^{\infty} e^{-s/\tau_{ch}} \left[h_1 |V(\tau - s)|^2 + h_2 |V(\tau - s)|^4 \right] ds$$

...due to carrier density changes

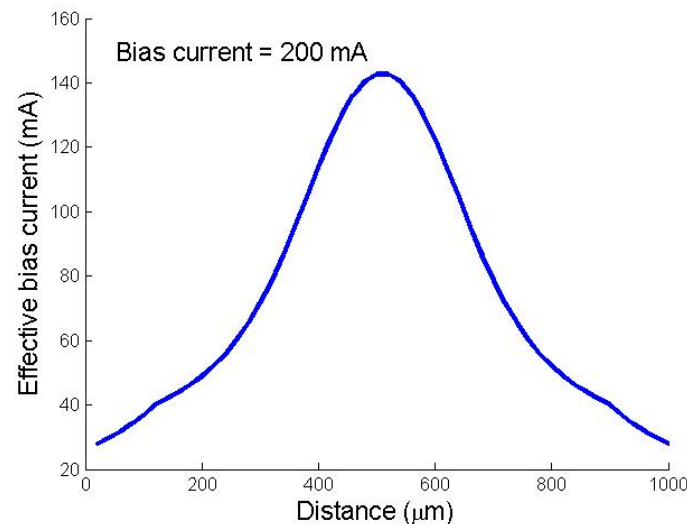
$g_n(z, \tau)$ is obtained from the solution to a *modified* carrier density rate equation

$$\frac{dn}{dt} = \frac{\eta(z)I_{eff}}{eV} - R(n) - \frac{\Gamma}{dW(z)} g_m(n) |V(z, \tau)|^2$$

$I_{eff}(z)$ is an effective spatially dependent bias current used to account for ASE. It is obtained by determining the spatially dependent SOA carrier density $n_0(z)$ for a given bias current and no input signal using a previously developed steady-state model* (includes ASE).

In this limit we have $dn/dt = 0$ so
$$I_{eff}(z) = \frac{R(n_0(z))eV}{\eta(n_0(z))}$$

This places the correct upper bound on the carrier density (and thereby the signal gain).



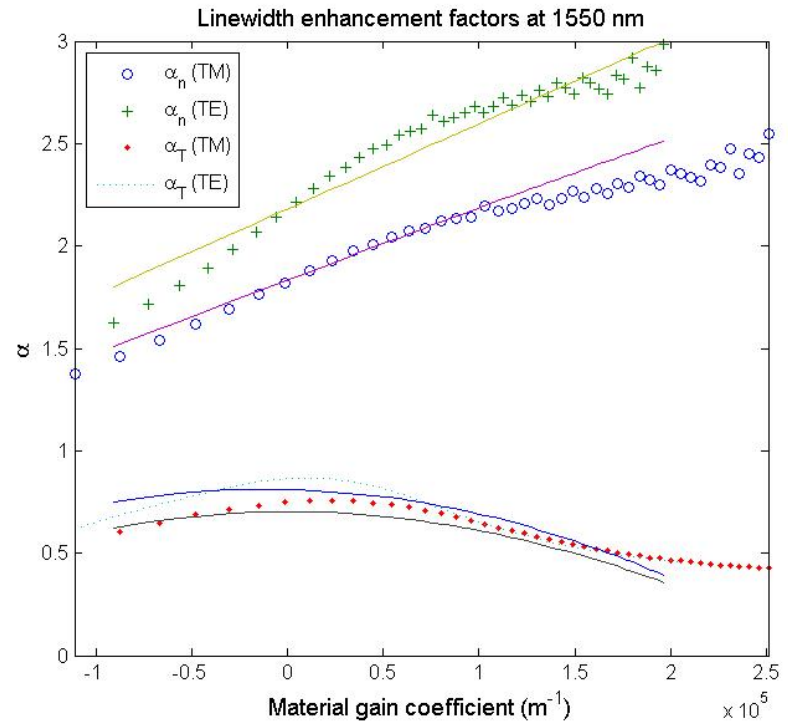
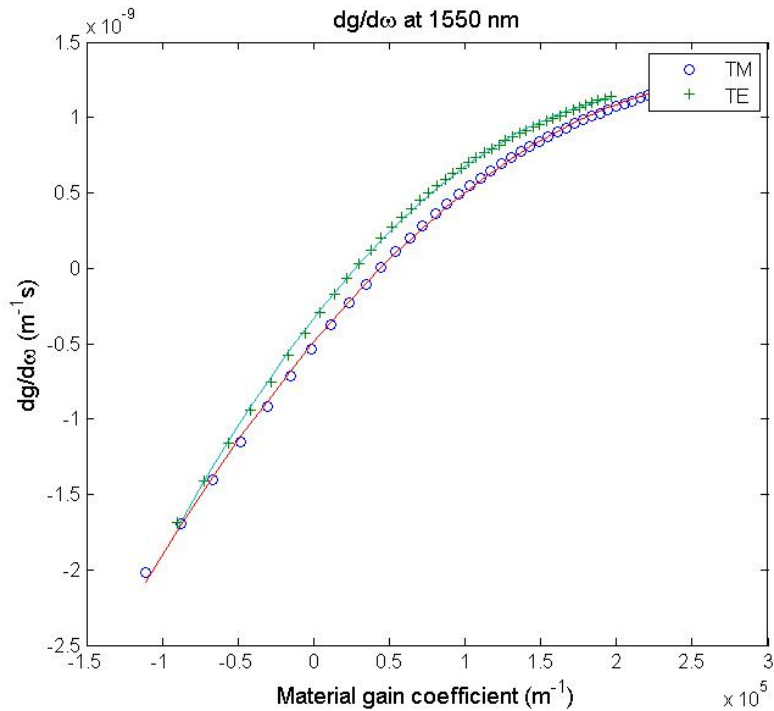
* M.J. Connelly, *IEEE J. Quantum Electron.*, Jan. 2007

$g_n(z, \tau)$ is modified by the spectral hole burning term $f(z, \tau) = 1 + \frac{|V(z, \tau)|^2}{P_{shb}}$

- Estimates of gain coefficient related quantities in the MSE (gain coefficient dispersion, linewidth enhancement factors and material gain coefficient) were obtained using the steady-state model and parameter extraction algorithm.
- In the MSE they are approximated as polynomial functions of the total dynamic gain, e.g.

$$\Gamma(z) \left. \frac{\partial g(z, \tau, \omega)}{\partial \omega} \right|_{\omega_0} = A(z) + B(z)g(z, \tau) + C(z)g(z, \tau)^2$$

- where A , B and C are the polynomial coefficients obtained from the plot of the quantity of interest versus material gain.



- Reasonable estimates of the MSE phenomenological constants (h_1 , h_2 etc.) were obtained by investigating the propagation of a stream of 2 ps wide pulses through the SOA using FROG and then solving the MSE in conjunction with the Levenberg-Marquardt parameter extraction technique*.

* M.J. Connelly et al. *13th Eur. Conf. Integ. Opt.*, 2007

Numerical algorithm and Simulations

- Solve the MSE using the finite difference beam propagation method to determine the complex envelope at the $j+1$ spatial step and $k+1$ time step*.

The finite difference approximation to the MSE is

$$-a_{j+1,k} V_{j+1,k-1} + (1 - b_{j+1,k}) V_{j+1,k} - c_{j+1,k} V_{j+1,k+1} = a_{j,k} V_{j,k-1} + (1 + b_{j,k}) V_{j,k} + c_{j,k} V_{j,k+1}$$

$$a_{j,k} = \frac{\Delta z}{2} \left[\frac{i}{4\Delta\tau} \frac{\partial g_{j,k}(\omega)}{\partial \omega} \Big|_{\omega_0} - \frac{1}{4\Delta\tau^2} \frac{\partial^2 g_{j,k}(\omega)}{\partial \omega^2} \Big|_{\omega_0} \right]$$

$$b_{j,k} = \frac{\Delta z}{2} \left[\left[\frac{\gamma_{j,k}}{2} + \left(\frac{\gamma_{2p}}{2} + ib_{2,j} \right) |V_{j,k}|^2 - \frac{1}{2} g_{n,j,k}(\omega_0)(1 + \alpha_{n,j,k}) - \frac{1}{2} \Delta g_{T,j,k}(\omega_0)(1 + \alpha_{T,j,k}) - \frac{1}{2\Delta\tau^2} \frac{\partial^2 g_{j,k}(\omega)}{\partial \omega^2} \Big|_{\omega_0} \right] \right]$$

$$c_{j,k} = -\frac{\Delta z}{2} \left[\frac{i}{4\Delta\tau} \frac{\partial g_{j,k}(\omega)}{\partial \omega} \Big|_{\omega_0} + \frac{1}{4\Delta\tau^2} \frac{\partial^2 g_{j,k}(\omega)}{\partial \omega^2} \Big|_{\omega_0} \right]$$

N.K. Das, et al. *IEEE J. Quantum Electron.*, 2000

- If the field at j is known then $V_{j+1,k+1}$ is determined first using the approximation.

$$V_{j+1,k+1}^0 = \left[2a_{j,k+1}V_{j,k} + (1 + b_{j,k+1})V_{j,k+1} + 2c_{j,k+1}V_{j,k+2} \right] (1 - b_{j,k+1})$$

The first order approximation to $V_{j+1,k+1}$ is then given by

$$V_{j+1,k+1}^1 = \left[a_{j+1,k}V_{j+1,k}^0 + a_{j,k+1}V_{j,k} + (1 + b_{j,k+1})V_{j,k+1} + c_{j+1,k+1}V_{j+1,k+2}^0 + c_{j,k+1}V_{j,k+2} \right] (1 - b_{j+1,k+1})$$

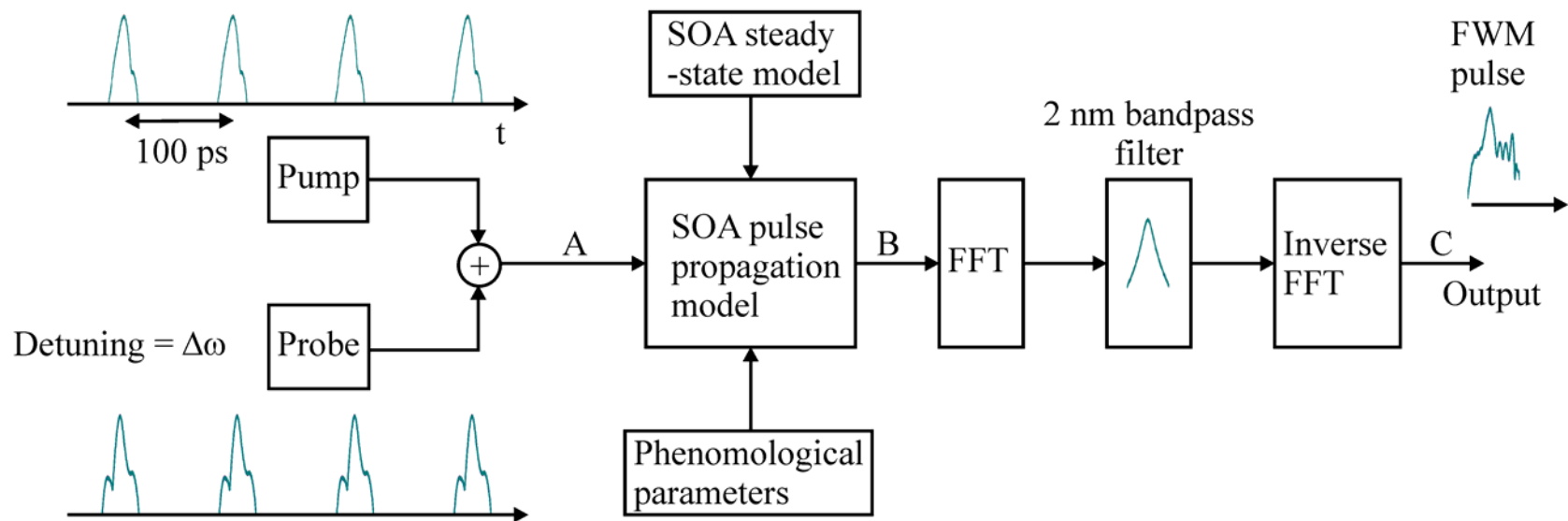
Because of the dominance of the $b_{j,k}$ type terms the algorithm is stable for appropriate values of the time and spatial steps

The *modified-Euler* finite difference technique is used to solve the carrier density rate equation, from which we obtain $g_n(z, \tau)$.

To model FWM the input pulse amplitude is $V_{in}(t) = V_{pump}(t) + V_{probe}(t) \exp(-j\Delta\omega t)$

Pump and probe have identical polarisations.

Complex amplitudes measured using FROG
 Detuning



Train of 6 pulses

Model schematic

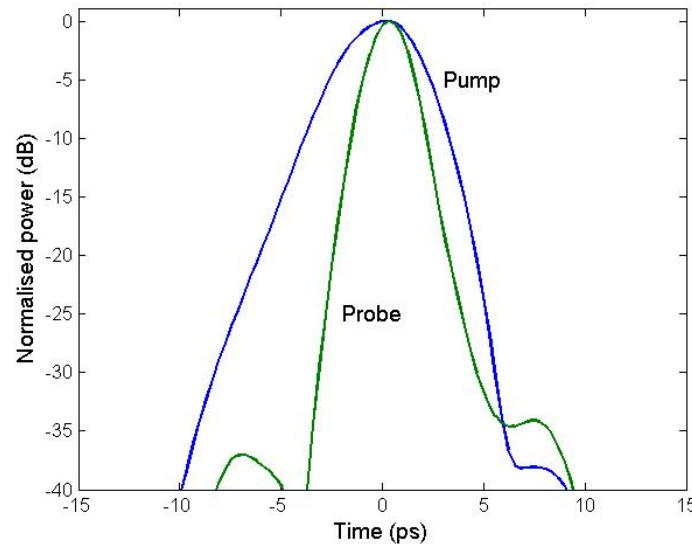
Pump and probe

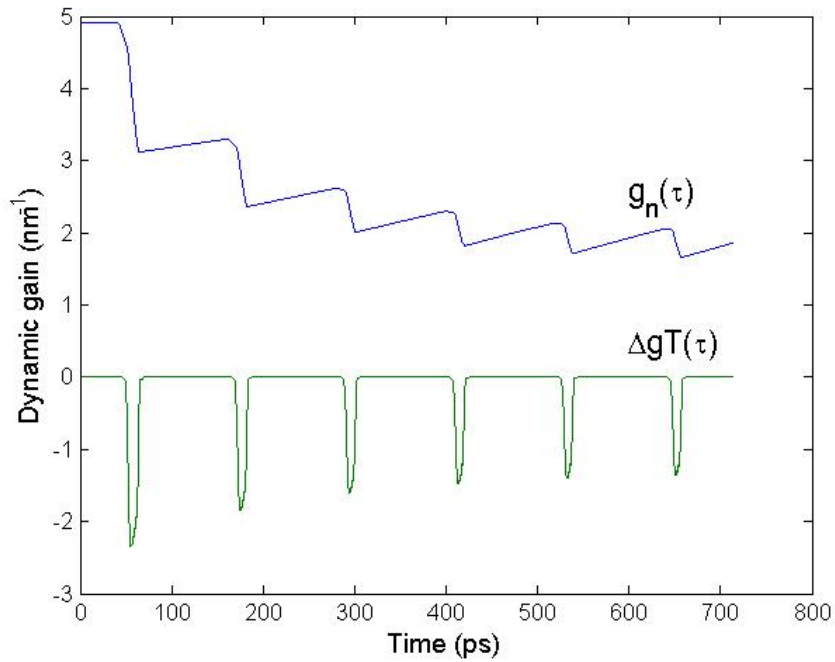
Pump peak power = 63 mW

Probe peak power = 5 mW

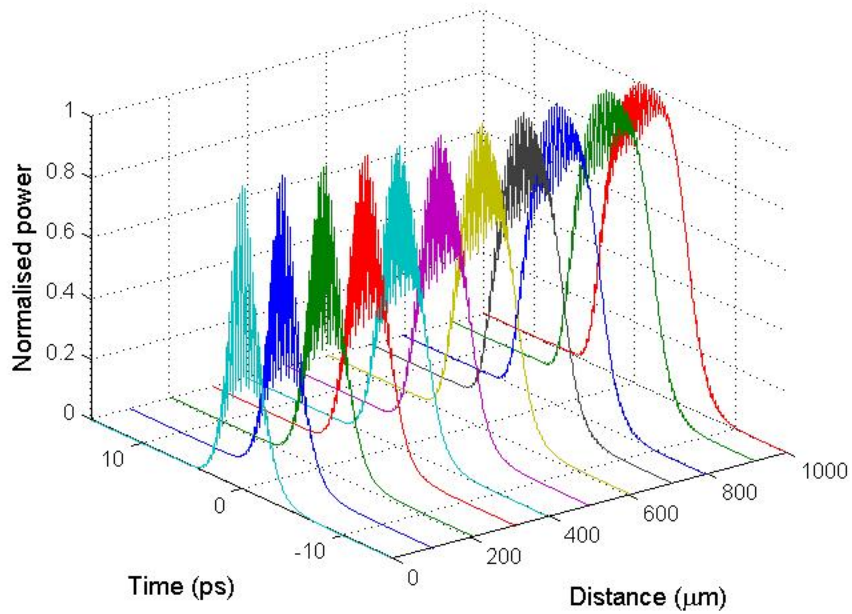
Pump pulse width ~ 4 ps

Probe pulse width ~ 2 ps



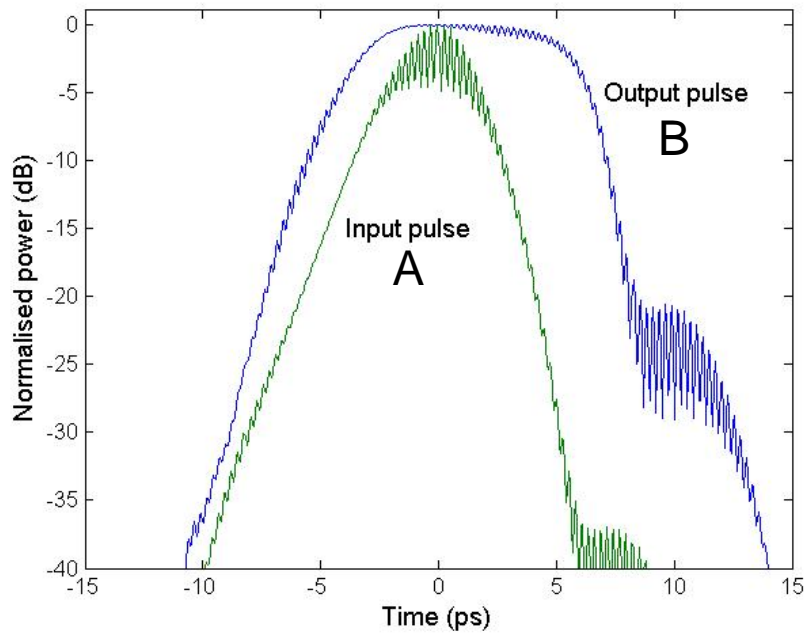


Dynamic gain

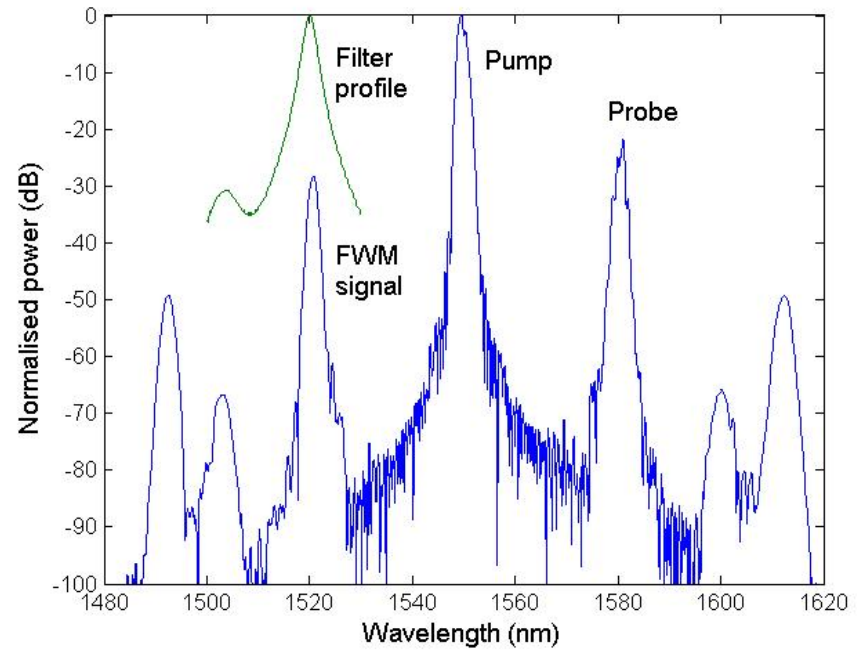


6th pulse at various positions in the SOA

Down-conversion (30 nm)



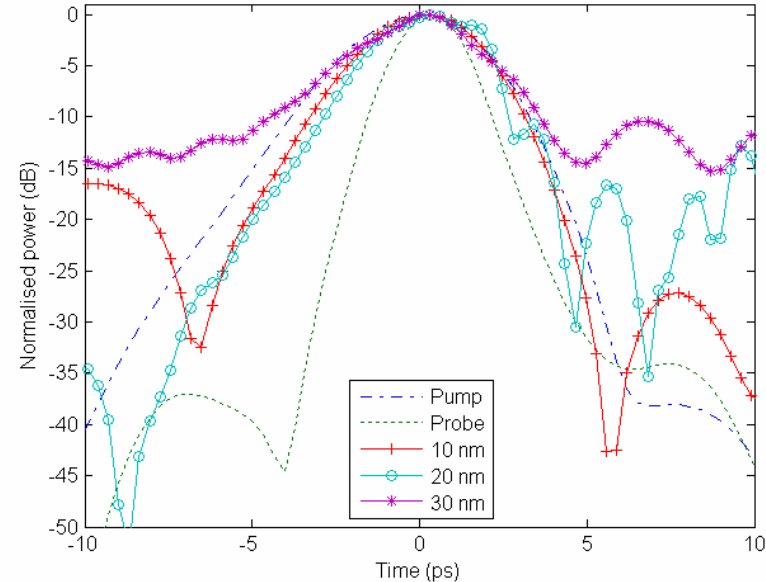
Input and output pulses



Output pulse spectrum

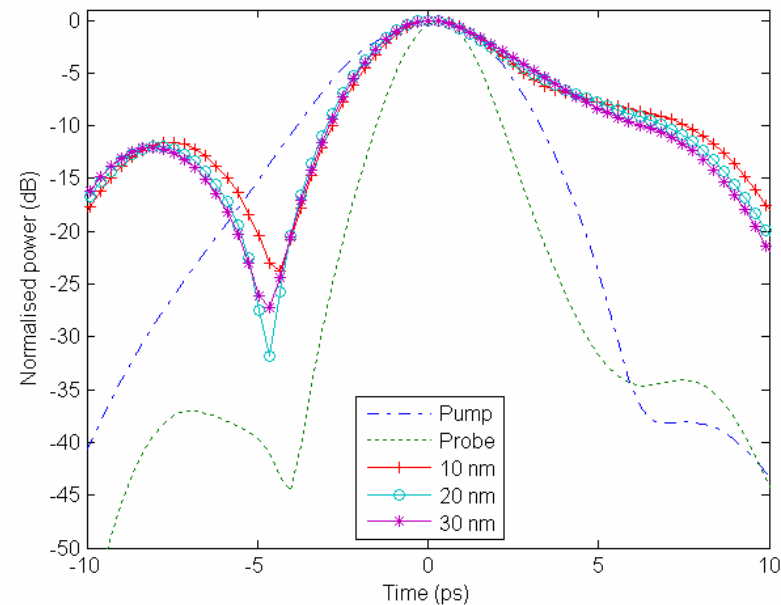
Experimental FWM pulse profile: down-conversion

Pedestal enhancement – leads to intersymbol interference



Simulated FWM pulse profile – pedestal enhancement predicted

FROG data not reliable at power levels > 30 dB below the peak power.



- Difficult to accurately predict exact FWM pulse profile over a large detuning range.
- Need to include in more detail the wavelength dependence of the dynamic gain.
- Will require modifications to the MSE.
- The explicit inclusion of forward and backward propagating ASE in the model will also be required.
- However this will require a much higher computation time.

Conclusions

- A numerical model of FWM between pump and probe picosecond pulses in a tensile strained bulk SOA has been developed
- Uses model parameters for a particular device obtained using a previously developed steady-state model and parameter extraction based on FROG experimental results.
- The model successfully predicts a large increase in the pedestals of the output FWM pulse.
- Future work will investigate the FWM pulse chirp and use the more accurate technique of frequency resolved electro-absorption gating to determine the fine structure of the pulses especially at power levels well below their peaks and use this information to improve the model.